International Journal of Innovative Research and Reviews, 10(1) 1-10

International Journal of Innovative Research and Reviews

ISSN: 2636-8919

Website: www.injirr.com

RESEARCH ARTICLE

Numerical Comparison of the Effect of Water-Based Nanofluid on the Performance of a Parabolic Solar Collector

Muhammet Kaan YEŞİLYURT*[1], Mansur MUSTAFAOĞLU[1]

[1] *Department of Mechanical Engineering, Engineering Faculty, Ataturk University, Erzurum, Türkiye*

* *Corresponding author E-mail: kaan.yesilyurt@atauni.edu.tr*

ARTICLE INFO

Received : 06.24.2025
Accepted : 02.18.2026
Published : 07.15.2025

Keywords:
Nanofluids
Parabolic Solar Collector
Heat Transfer
CFD
Numerical Simulation

ABSTRACT

This study presents a comprehensive numerical analysis of the thermal performance enhancement achieved by incorporating water-based nanofluids into parabolic solar collector systems. The nanofluids were formulated by dispersing titanium dioxide (TiO_2) and aluminum oxide (Al_2O_3) nanoparticles into deionized water at defined volume fractions. Numerical simulations were conducted using the finite volume method (FVM) on a three-dimensional parabolic trough collector, employing a structured mesh composed of 70 radial and 2000 axial nodes. Boundary conditions included an inlet temperature of 25°C, incident solar radiation of 1000 W/m², and a natural convection coefficient of 6.43 W/m²K. The results demonstrate that the incorporation of TiO_2 at a 0.03% volume fraction led to an enhancement in outlet temperature and thermal efficiency of up to 12% compared to the base fluid. Although a marginal increase in viscosity was observed, the nanofluid yielded a more uniform thermal profile and improved convective heat transfer. Parametric studies further revealed a direct linear relationship between flow rate and thermal output, along with a saturation behavior in thermal conductivity at elevated nanoparticle concentrations. Overall, the findings substantiate the efficacy of TiO_2 and Al_2O_3 enhanced nanofluids in enhancing the thermal performance of parabolic solar collectors and provide valuable insights for optimizing next-generation solar thermal energy systems.

Contents

1. Introduction 2
2. Materials and methods 2
   2.1. Problem definition 2
   2.2. Computational Methodology 3
      2.2.1 Geometric Model and Computational Domain 3
      2.2.2 Assumptions and Governing Equations 3
      2.2.3 Boundary Conditions 3
      2.2.4 Nanoparticles and Nanofluid Properties 4
      2.2.5 Numerical Solution and Convergence Criteria 4
      2.2.6 Meshing 5
      2.2.7 Mesh Quality and Grid Independence 5
3. Results and Discussion 6
4. Conclusion 9
Limitations 9
Future Research 10
Conflict of interest 10
Author Contributions 10
References 10

Cite this article Yeşilyurt MK, Mustafaoğlu M. Numerical Comparison of the Effect of Water-Based Nanofluid on the Performance of a Parabolic Solar Collector. *International Journal of Innovative Research and Reviews (INJIRR)* (2026) 10(1) 1-10

Link to this article: http://www.injirr.com/article/view/246

1. Introduction

The increasing global energy demand and the imperative to reduce carbon emissions have spurred innovative research in renewable energy technologies, particularly solar energy systems. Among these technologies, concentrated solar power (CSP) systems, and parabolic trough solar collectors (PTSCs), are notable for their capacity to efficiently generate heat at high temperatures. However, the overall performance of these systems is constrained by the limited thermophysical properties of traditional heat transfer fluids (HTFs) such as water or glycol, particularly their low thermal conductivity. To overcome these limitations, a new generation of fluids developed through the integration of nanotechnology into thermal systems, called nanofluids, offer enhanced thermal transport capabilities.

Nanofluids are engineered colloidal suspensions created by stably dispersing metal (e.g., Al, Cu), metal oxide (e.g., Al_2O_3, TiO_2, CuO), or carbon-based nanoparticles into conventional host fluids like water or oil. These advanced fluids overcome the thermal limitations of conventional base fluids by significantly improving thermal conductivity, thereby increasing efficiency across various energy systems, including parabolic solar collectors, heat pipes, and electronic cooling applications. Recent literature consistently highlights the efficacy of these suspensions in enhancing thermal energy conversion and heat dissipation at elevated temperatures; both individual metal oxide dispersions and hybrid combinations (such as Cu-TiO_2) have demonstrated significant thermal and mass transfer improvements under varying operational conditions [1, 2]. The enhanced synergetic effect observed in these fluids is primarily governed by complex particle-fluid interactions and host fluid compatibility rather than solely the nanoparticle material.

While metal oxide nanoparticles are widely used, carbon-based materials such as graphene and carbon nanotubes (CNTs) are also attracting attention due to their exceptional thermal conductivity. However, their tendency to agglomerate, long-term stability issues, and potential environmental impacts limit their practical applications. For these reasons, metal oxide-based nanofluids are often preferred because they offer a balanced optimization between performance, availability, and cost.

The thermophysical behavior of nanofluids (thermal conductivity, viscosity, specific heat) does not scale linearly with particle concentration; rather, it exhibits non-linear dependencies driven by particle morphology, size, and fluid-particle interactions.

One of the most significant challenges associated with the use of nanofluids is the trade-off between increased heat transfer and increased pumping power. While nanofluids improve thermal performance, they also increase system viscosity. This requires increased pump power to circulate the fluid and increases operating costs. Research shows that, beyond a certain nanoparticle concentration, the marginal gain in heat transfer does not offset the hydraulic losses introduced by the increased viscosity. Therefore, determining the optimal particle concentration is essential to achieve maximum thermal efficiency with minimal energy consumption.

Beyond improving performance, nanofluids provide a more uniform temperature distribution throughout the absorber tube, reducing thermal stress and extending system life. This temperature stability increases system reliability, particularly under conditions of variable solar irradiance or partial shading. Furthermore, a stable temperature profile facilitates thermal energy storage processes, which are critical for integrating generated energy into the grid.

While the literature emphasizes the importance of Computational Fluid Dynamics (CFD) simulations, it also reveals that experimental validation is indispensable because these models often rely on idealized assumptions and cannot fully capture complex multiphase interactions. Experimental validation remains necessary to confirm that MgO nanofluids practically provide the performance improvements predicted theoretically. Therefore, an integrated approach combining numerical modeling and experimental validation offers the most robust methodology for advancement in the field [3].

To maximize the efficiency of these thermal systems, researchers emphasize the necessity of comprehensive, multidisciplinary optimization. Thermodynamic evaluations, such as entropy generation analysis, play a critical role in predicting fluid flow behavior and maximizing overall system efficiency [4]. Furthermore, literature dictates that factors including material selection, surfactant application, and specific collector geometry must be integrated holistically to achieve optimal performance [5, 6]. Despite their proven application potential, the widespread commercial implementation of nanofluids remains constrained by ongoing challenges related to long-term colloidal stability, economic feasibility, and environmental impacts, which continue to be active areas of investigation [7–11] .

This study aims to numerically assess the influence of TiO_2 and Al_2O_3 based nanofluids on the thermal performance of parabolic solar collectors. Emphasis is placed on optimizing collector efficiency by evaluating key parameters such as nanoparticle volume fraction, fluid flow rate, and absorber length through a CFD-based framework. The findings are expected to provide theoretical insights for the design of next-generation nanofluid-integrated solar thermal systems.

2. Materials and methods

2.1. Problem definition

Improving the thermal efficiency of parabolic trough solar collectors (PTSCs) is one of the key research challenges for the widespread adoption of this technology. The limited thermophysical properties of conventional heat transfer fluids are considered one of the main factors limiting system performance. In this context, this study aims to numerically investigate the effects of using water-based Titanium Dioxide (TiO_2) and Aluminum Oxide (Al_2O_3) nanofluids as heat transfer fluids in PSC systems on thermal and hydraulic performance.

The primary objective of this study is to comprehensively analyze how different nanoparticle types and concentrations affect collector efficiency under various flow regimes and absorber tube geometries. For this purpose, a three-dimensional simulation model based on Computational Fluid Dynamics (CFD) was developed. The primary objectives of the study are to:

– quantitatively determine the effect of water-based TiO_2 and Al_2O_3 nanofluids on the heat transfer coefficient and overall thermal efficiency of the POGK system compared to pure water.

– parametrically study the individual and combined effects of key design and operating parameters such as nanoparticle volumetric concentration (in the range of 0.01%–0.05%), flow rate (represented by Reynolds number), and absorber tube diameter on system performance.

– make an assessment of the overall effectiveness of the system by analyzing the improvement in thermal performance as well as the increase in pressure drop and pumping power requirement caused by nanofluid.

Numerical simulations were performed under defined boundary conditions to reflect real-world operating conditions.

2.2. Computational Methodology

2.2.1 Geometric Model and Computational Domain

The three-dimensional (3D) parabolic trough solar collector (PTSC) system used for performance analysis consists mainly of a parabolic reflective surface, an absorbent pipe placed on the focal line of the reflector, and a support structure bearing these components. The solar irradiance is collected by the parabolic reflector to focus on the outer surface of the absorber tube and increase the temperature of the heat transfer fluid in the pipe.

A 3D model was chosen to accurately capture both the heat transfer across the absorber tube's cross-section and the progressive temperature increase of the fluid along the axial direction of the collector. The absorbent tube is modelled as a cylindrical tube with a diameter of 160 mm and a length of 2 m, featuring a 12-point star shaped groove in the center along the length to enhance heat transfer and flow characteristics and eventually improve the collector's thermal efficiency by maximizing the heat absorption capacity of the nanofluid and increasing the convective heat transfer coefficient.

The schematic view of the system is presented in Figure 1.

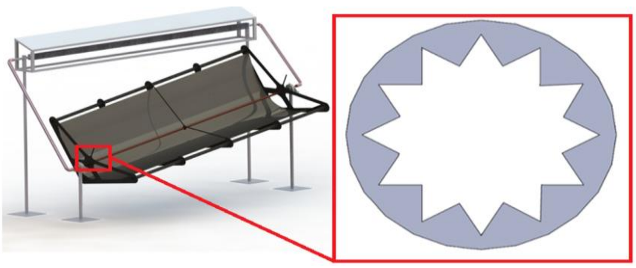

Figure 1 Three-dimensional view of the parabolic collector and the pipe

The tip angle of each fin is determined as 90° and the base width of the fins is 25 mm while the diameter of the circular space formed by the end points of the fins is 100 mm.

2.2.2 Assumptions and Governing Equations

The fluid dynamics model was based on the assumptions that the flow is laminar, steady-state, incompressible and continuous. The effects of radiation and viscous losses were neglected.

In this regard, the problem is governed by the continuity equation, customized set of Navier-Stokes equations which describe the motion due to net forces on the fluid, and the energy equation with Boussinesq approximation.

The conservation of mass, which is also known as the continuity equation is expressed as:

$$\frac{\partial u}{\partial x}+\frac{\partial v}{\partial y}+\frac{\partial w}{\partial z}=0 \quad (1)$$

The Momentum equations are as follows with the Boussinesq approximation which assumes that the density variations are only considered for the effects of buoyancy due to free convection:

$$\rho_{nf}(u\frac{\partial u}{\partial x}+v\frac{\partial u}{\partial y}+w\frac{\partial u}{\partial z}) = -\frac{\partial P}{\partial x}+\mu_{nf}(\frac{\partial^2 u}{\partial x^2}+\frac{\partial^2 u}{\partial y^2}+\frac{\partial^2 u}{\partial z^2}) \quad (2)$$

$$\rho_{nf}(u\frac{\partial v}{\partial x}+v\frac{\partial v}{\partial y}+w\frac{\partial v}{\partial z}) = -\frac{\partial P}{\partial y}+\mu_{nf}(\frac{\partial^2 v}{\partial x^2}+\frac{\partial^2 v}{\partial y^2}+\frac{\partial^2 v}{\partial z^2}) \quad (3)$$

$$\rho_{nf}(u\frac{\partial w}{\partial x}+v\frac{\partial w}{\partial y}+w\frac{\partial w}{\partial z}) = -\frac{\partial P}{\partial z}+\mu_{nf}(\frac{\partial^2 w}{\partial x^2}+\frac{\partial^2 w}{\partial y^2}+\frac{\partial^2 w}{\partial z^2})+\rho_{nf}g\beta(T-T_{ref}) \quad (4)$$

The conservation of energy is expressed as:

$$\rho_{nf}\, C_{P,nf}\left(u\frac{\partial T}{\partial x}+v\frac{\partial T}{\partial y}+w\frac{\partial T}{\partial z}\right) = k_{nf}\left(\frac{\partial^2 T}{\partial x^2}+\frac{\partial^2 T}{\partial y^2}+\frac{\partial^2 T}{\partial z^2}\right) \quad (5)$$

2.2.3 Boundary Conditions

The initial temperature of the parabolic solar collector used in the study was assumed to be equal to the ambient temperature. The initial velocities of the nanofluid (water-based aluminum oxide and titanium dioxide nanoparticles) and pure water were defined at a constant inlet velocity for each analyzed scenario. The radiation flux on the collector surface was taken as 1000 W/m², and the spectral distribution of solar radiation was modeled in the wavelength range of 0.2-6 µm. The heat transfer coefficient (convection) on the outer surface of the collector was determined to be 6.43 W/m²K, and the ambient temperature was assumed to be constant at (25°C. It is assumed that the nanofluid and pure water are in a laminar flow regime. At the inlet and outlet boundaries, the pressure gradient was defined as zero, and the flow rate was varied in the range of 0.1-0.8 m/s in the parametric analysis. The thermophysical properties of the nanofluid (thermal conductivity, specific heat, and density) were calculated using the mixture rule. The diameter of the Al_2O_3 and TiO_2 nanoparticles were taken as 40 nm, and their volumetric ratio varied between 0.02% and 0.4%. A single-phase modeling approach was adopted assuming that the nanofluids form a homogeneous suspension.

These conditions have been defined to ensure the accuracy of the numerical model and to isolate the impact of different parameters on performance.

2.2.4 Nanoparticles and Nanofluid Properties

While water is widely used in heat transport systems due to its high specific heat capacity and low viscosity, oxide-based nanoparticles such as aluminum oxide (Al_2O_3) are frequently preferred in nanofluid systems due to their high thermal conductivity and chemical stability. Incorporation of Al_2O_3 induces significant changes in these properties of the fluid. For example, with Al_2O_3 addition, the density and viscosity of the liquid increase, while a decrease in specific heat capacity can be observed. However, as a result of these changes, the heat conductivity of the overall system increases significantly, which provides a significant advantage in drawing more heat from the system.

Table 1 Physical properties of nanofluid and water at 26ºC [12–14].

Property	Water	Al_2O_3	TiO_2
μ (kg/m.s)	1.002×10^{-3}	-	-
ρ (kg/m³)	998.3	3600	4250.0
β (1/K)	0.207×10^{-3}	8.46×10^{-6}	8.4×10^{-6}
k (kW/mK)	0.598×10^{-3}	12	8.4
C_p (kJ/kgK)	4.179	0.765	0.686

Evaluating the thermal performance of high-density nanofluid systems is highly dependent on the physical properties of the nanoparticles used. These properties include parameters such as particle size, morphology, specific heat capacity, thermal conductivity, and density. The physical properties of nanoparticles are presented in Table 1.

The data given in Table 2 show that the effective (composite) thermophysical properties of nanofluids calculated with appropriate theoretical models.

Determination of the effective thermophysical properties plays a critical role in predicting the heat transfer efficiency, pumping power requirements, and hydraulic performance of the nanofluid. The behavior of the system under real operating conditions directly influences the accuracy of the effective properties used in numerical modeling. At this point, the validity of the model can be reinforced by testing the compatibility of the parameters used in it with experimental studies in the literature.

Table 2 Physical properties of Al_2O_3 /water and TiO2 /water [13, 14]

Physical properties	TiO2 /water	Al_2O_3 /water
μ_{nf} (kg/ms)	0.95×10^{-3}	1.3508×10^{-3}
ρ_{nf} (kg/m³)	1060.33	1076.3510
$\rho_{nf}\beta_{nf}$ (kg/m³K)	0.2001	0.2013
k_{nf} (kW/mK)	0.65×10^{-3}	0.6614×10^{-3}
$\rho_{nf}Cp_{bf}$(kJ/m³K)	4000.7537	4129.3588

Due to the low nanoparticle concentration and stable particle distribution, the nanofluid was modeled as a single-phase fluid, and its effective thermophysical properties were used:

$$\rho_{\mathrm{nf}} = (1-\varphi)\rho_{\mathrm{f}} + \varphi\rho_{np} \tag{6}$$

$$\rho_{nf}C_{\mathrm{p,nf}} = (1-\varphi)\rho C_{\mathrm{p,f}} + \varphi\rho C_{\mathrm{p,np}} \tag{7}$$

$$\beta_{\mathrm{nf}} = (1-\varphi)\beta_{\mathrm{f}} + \varphi\beta_{np} \tag{8}$$

The effective thermophysical properties of the NFs are calculated as given above. Viscosity (μ) come from chosen Brinkman mixture model, and thermal conductivity (k) from Maxwell correlation, which respectively given as:

$$\mu_{nf} = \mu_f(1-\phi)^{-2,5} \tag{9}$$

$$k_{nf} = k_f\frac{k_p + 2k_f - 2\phi(k_f - k_{np})}{k_p + 2k_f + \phi(k_f - k_{np})} \tag{10}$$

2.2.5 Numerical Solution and Convergence Criteria

To numerically investigate the thermal performance of the absorber tube within a PTSC using water-based nanofluids, the Finite Volume Method (FVM) was employed. FVM was selected for its local conservation properties and its capability to accurately resolve fluid-solid heat transfer, as well as simultaneous radiative and convective heat transfer, within complex mesh structures. Consequently, the commercial computational fluid dynamics (CFD) software ANSYS Fluent was utilized for all numerical simulations. For the discretization of the governing equations, the Semi-Implicit Method for Pressure-Linked Equations (SIMPLE) algorithm was chosen to resolve the strong coupling between the pressure and velocity fields in the steady-state flow. To minimize numerical diffusion and improve computational accuracy, a Second-Order Upwind scheme was applied to the transport terms within the momentum and energy equations. Convergence of the numerical solution was evaluated using both mathematical and physical stability criteria. All normalized residual values calculated for the continuity, momentum, and energy equations were required to fall strictly below a threshold of 10^{-6}. In addition to satisfying the residual criterion, physical parameter stability was monitored throughout the iterations. The solution was deemed fully converged only when the average surface temperature of the absorber tube and the mass-weighted average outlet temperature of the fluid reached a constant value, ensuring the results were both mathematically and physically reliable.

2.2.5.1 Data Reduction and Performance Metrics

In order to optimize the system performance, the effects of four key parameters were investigated: concentration ratio (C), nanoparticle volume fraction (ϕ), absorber tube length (L) and fluid flow rate (Q). The impact of each parameter was evaluated on key performance metrics such as average outlet temperature, thermal efficiency and optical efficiency.

The heat absorption rate is the measure of the useful thermal energy gained by the working fluid as it flows through the collector. It is calculated from the fluid's mass flow rate and the change in its bulk temperature between the inlet and outlet.

$$\dot{Q} = \dot{m}\, C_{p,nf}\, (T_{out} - T_{in}) \tag{11}$$

Here, $\dot{m}$ is the mass flow rate and $C_{p,nf}$ is the effective specific heat of nanofluid; T_{in} is the uniform temperature at the collector inlet (K) and T_{out} mass-flow-weighted average temperature at the collector outlet (K), obtained directly from the CFD results to ensure accuracy.

Since the heat drawn from the pipe wall is transferred to the fluid:

$$\dot{Q} = h_i A_i \Delta T_{lm} \tag{12}$$

Here, h_i is the overall heat transfer coefficient along the absorber tube, A_i is the heat transfer surface area for the nanofluid, and ΔT_{lm} is the logarithmic temperature difference between the wall and the fluid in contact with the wall, which is expressed as:

$$\Delta T_{lm} = \frac{\Delta T_{wall} - \Delta T_{fluid}}{\ln\left(\frac{\Delta T_{wall}}{\Delta T_{fluid}}\right)} \tag{13}$$

Once h_i is obtained, Nusselt number is calculated using:

$$Nu = h\, D_h / k_{nf} \tag{14}$$

where k_{nf} denotes the effective thermal conductivity of the nanofluid, and D_h is the hydraulic diameter of the absorber tube.

As a final measure of the system's performance, thermal efficiency is calculated as the ratio of the useful thermal energy absorbed by the fluid to the total solar energy incident on the collector's aperture:

$$\eta = \frac{Q}{A_a\, G} \tag{15}$$

where G is the incident solar irradiance in W/m^2, which is 1000 W/m² for the present study.

2.2.6 Meshing

Solution meshes are created in two ways depending on the geometric properties: structured and unstructured. We create structured solution meshes in an orderly manner by considering specific geometric properties. Structured solution networks yield results with a low margin of error, that are more accurate and easier to understand and interpret. In the study, a structured solution mesh was preferred, allowing for the regular and symmetrical distribution of node points. This approach contributes to a more accurate modeling of fluid motion and heat transfer processes.

On the other hand, unstructured solution meshes are created randomly without adhering to geometry and generally have a more flexible structure. They are often used in complex geometries and variable boundary conditions and allow for a broader perspective in addressing the model. However, they may lead to a higher margin of error.

Both approaches have their advantages and disadvantages, and the correct choice is critical for the success of the application.

As a rule of thumb for CFD meshing in heat transfer analysis, velocity-based dimensionless wall distance, y^+ was chosen as the critical factor to consider during mesh setup. The required first cell distance from the wall was estimated using:

$$y1 = \frac{y^+ \cdot \mu}{\rho \cdot u_T} \tag{16}$$

where μ is dynamic viscosity, ρ is the density and u_T is the friction velocity. In order to resolve the viscous sublayer, the y^+ parameter was intended to be between 1 and 5. Accordingly, the final mesh was estimated to have some 30M elements.

2.2.7 Mesh Quality and Grid Independence

Five different mesh resolutions were tested ranging from 10M element coarser mesh to 25M finest.

For all mesh configuration, the temperature and the y+ parameter were monitored and the respective variation in the parameter was recorded in order to ensure that the solution was independent from the mesh size. In the courser mesh the average y^+ was greater than 10 and improved to somewhere between 2 and 3 in the finest configuration whereas the respective percent change in the temperature fell well under %1 with %0.1 in the finest and %0.2 in the finer configurations, detailed in Table 3 and Figure 2 below.

Table 3. Grid independence evaluation table

	Coarser	Coarse	Fine	Finer	Finest
Mesh Size	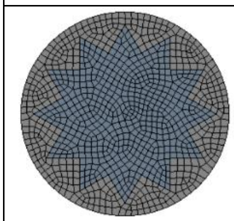	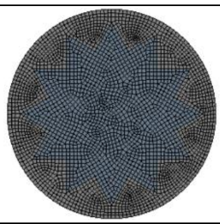	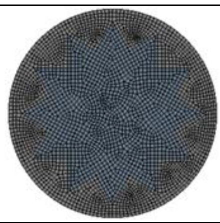	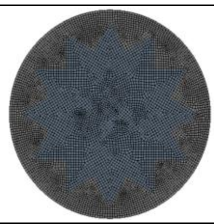	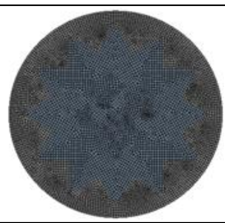
# of Cells	10,588M	17,647M	24,706M	31,765M	35,294M
Avg y+	>10	>5	~5	2–3	2–3
Ch% in T	%–	%4.2	%2.1	%<1	%<1

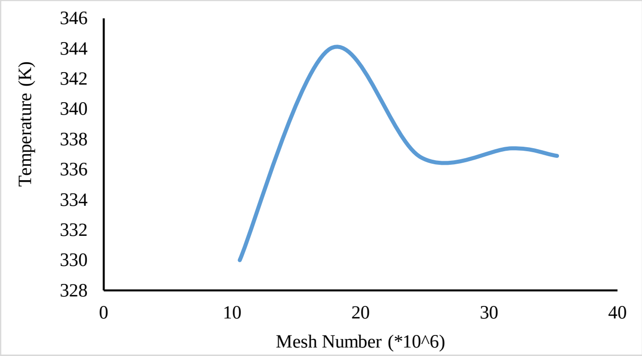

Figure 2 Grid independence test

Considering the marginal improvement and the additional computational cost, the finer mesh with 31.8M elements was used for the analyses. Figure 3 show the three-dimensional meshed model of the absorber tube.

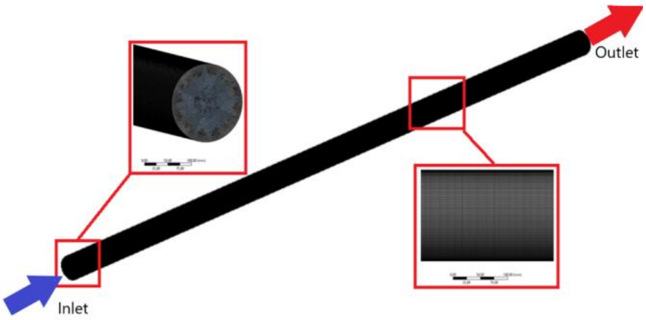

Figure 3 The mesh created for the double-tube heat exchanger a) Three-dimensional view b) Meshed section of the analysis area

The maximum skewness ratio for the final mesh was determined to be 0.672, and it was observed that the majority of the skewness ratios concentrated in the range of 0.08 to 0.25. This distribution indicates that the quality of the mesh is high and that the probability of a numerical error in the solution is low. This level of mesh quality is particularly critical in the study of turbulence and boundary layer behavior of nanofluids. The high-resolution mesh structure particularly increased computational accuracy in regions with high temperature and velocity gradients by allowing for the full utilization of the computational advantages offered by finite volume-based simulation.

3. Results and Discussion

TiO_2 and Al_2O_3 nanoparticles were incorporated into water at seven different volumetric concentrations to evaluate the effects of TiO_2 and Al_2O_3 nanofluids on the thermo-hydraulic performance of a PTSC system and to determine their advantages compared to water. Altering the physical properties of working fluid alters the heat transfer coefficient. The dispersion of nanoparticles in water significantly increases the thermal conductivity of the fluid as well as the heat transfer surface area. The analyses first evaluate the performance of each nanofluid compared to pure water and with each other.

In Figure 4, a comparison of the outlet temperatures obtained from solar collectors using pure water and water-based nanofluid (specifically TiO_2 and Al_2O_3 doped) is presented. The outlet temperature has significantly increased with nanofluids compared to pure water. This increase is due to the enhanced thermal conductivity properties of the nanofluid. Nanoparticles, due to their high thermal conductivity and increased surface area-to-volume ratio, absorb thermal energy from the inner pipe wall more efficiently, enhancing the overall convective heat transfer rate. Additionally, the micro-dynamic movements of the particles within the nanofluid enhance the heat transfer mechanisms, resulting in a more homogeneous temperature distribution and higher energy transfer.

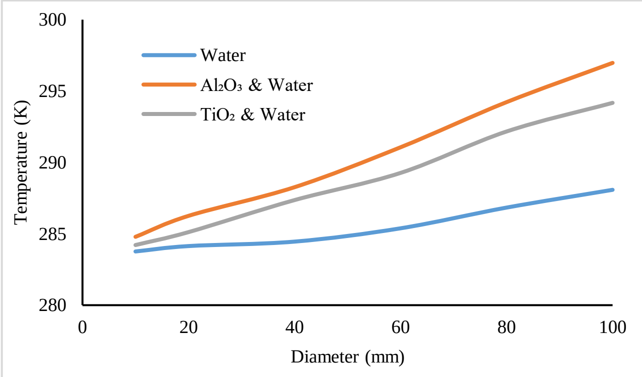

Figure 4 Outlet temperature for collectors containing water and nanofluid

Using optimized nanoparticle-enhanced fluids instead of pure water in solar collectors offers a viable method for enhancing system efficiency. Especially at low concentrations, the performance contribution of nanofluids strengthens the potential for using these materials in solar energy applications. This increase in outlet temperature also enables faster charging of thermal energy storage systems and enhances the overall system capacity.

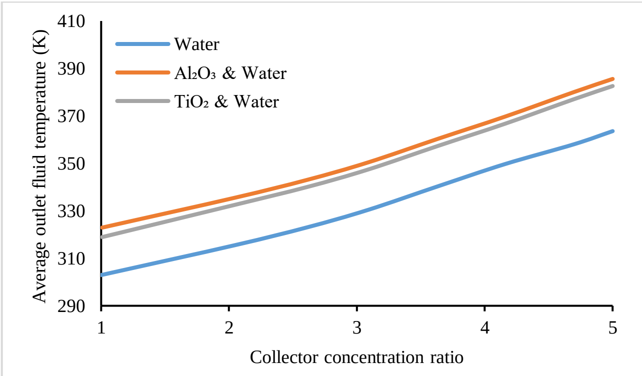

Figure 5 Average liquid outlet temperature according to collector concentration

Figure 5 shows the effect of nanoparticle concentration (volumetric ratio) in the nanofluid on the average outlet temperature. The average outlet temperature increases with concentration ratio due to the respective increase in heat transfer capacity resulting from the rise in the number of particles. The trend shows a saturation tendency after a certain concentration level where additional particles do not make a significant contribution to heat transfer.

This finding indicates that determining the optimal concentration in the design of nanofluid systems is a critical engineering decision. High concentrations can increase viscosity, leading to flow resistance, so a balance must be struck between efficiency and pumping cost..

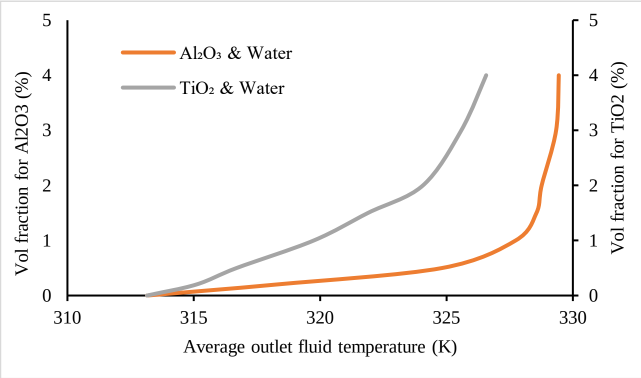

Figure 6 The ratio of the average liquid outlet temperature to the nanoparticle volume

Figure 6 shows the variation of the average liquid outlet temperature according to the nanoparticle volume fraction in the used nanofluid. A significant increase in outlet temperature is with TiO_2-nanofluid. Especially between the volume fractions of 0.02% and 0.08%, the outlet temperature shows an increase of approximately 2-3°C, indicating an improvement in heat transfer efficiency of 5% to 10%. This increase is due to the nanoparticles enhancing thermal conductivity, thereby improving the heat transfer capacity within the liquid. However, the curve reaching saturation at high volume fractions indicates that the system is approaching its maximum efficiency level. This saturation indicates that adding more nanoparticles limits the potential to increase heat transfer. Additionally, since an increase in viscosity occurs at high concentrations, pumping power and system energy consumption should also be taken into account. In conclusion, determining the optimum nanoparticle ratio is critically important for both thermal efficiency and system sustainability.

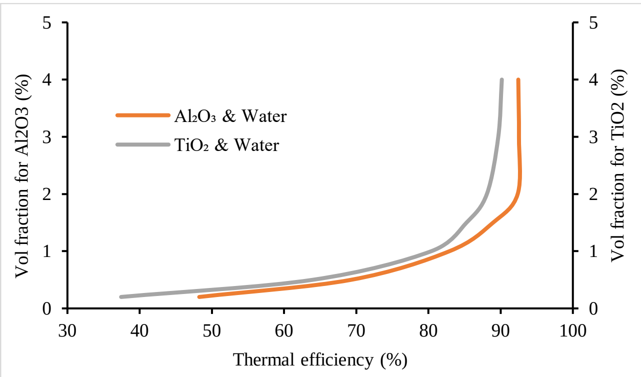

Figure 7 The ratio of thermal efficiency to the nanofluid volume ratio

Figure 7 shows the effect of the volumetric ratio of nanofluids on the thermal efficiency of the collector. According to the graph data, when the volumetric ratio of TiO_2 water-based nanofluids is increased from 0.5% to 1%, the thermal efficiency rises from approximately 69% to 80.3%. This linear increase is due to the high thermal conductivity of the nanoparticles providing a more homogeneous temperature distribution within the fluid and transporting heat more effectively. However, for both TiO_2 and Al_2O_3, the thermal efficiency increases as the concentration rises up to 2%. However, beyond this point, the increase in efficiency has slowed down and converged to a constant around 90%. This is more evident in Al_2O_3.

The most significant drawback related to increased NP concentration is the sharp increase in the fluid's dynamic viscosity which, in return, leads to a thicker viscous sublayer that hinders convective heat transfer and requires significantly more pumping power in a real-world application.

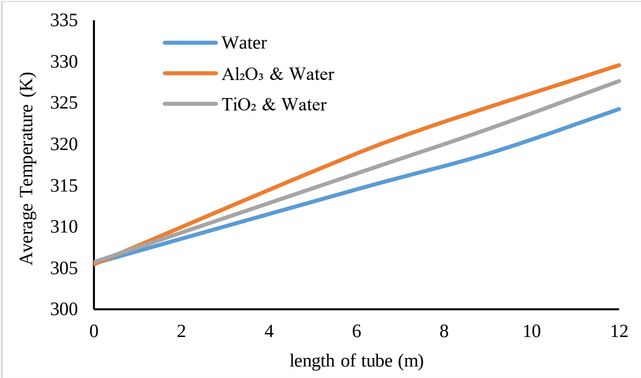

Figure 8 Average liquid temperature along the pipe length

Figure 8 shows the average liquid temperature along the length of the pipe. In systems using nanofluids, it is observed that the fluid temperature shows a regular increase from the beginning to the end and is approximately 7–10°C higher at the outlet compared to conventional water. For example, at the end of a 2-meter-long pipe, the TiO_2-water nanofluid reaches approximately 57°C, while pure water remains around 47°C. This confirms that the nanofluid can absorb more energy from solar radiation and has higher convective conductivity.

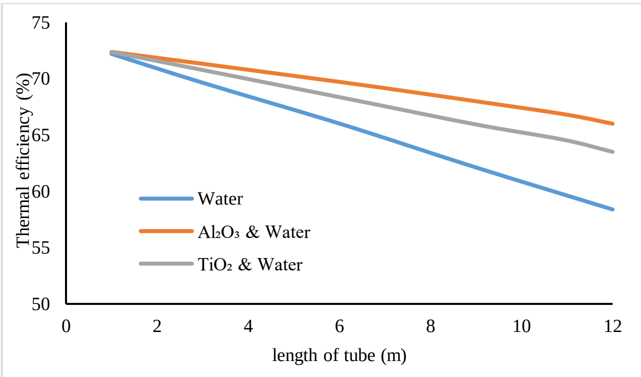

Figure 9 Thermal efficiency along the pipe length

Figure 9, on the other hand, shows the thermal efficiency of the system along the same pipe length. In systems operating with nanofluids, the efficiency starts at 55% and increases to levels around 67%, with this increase being particularly noticeable in the first 1.5-meter section. This situation indicates that higher temperature gradients are formed initially and that the heat transfer rate reaches its maximum level. In the final section, the slowdown in efficiency increase indicates that the system is approaching thermal equilibrium and that the temperature differences are decreasing. Overall, these three graphs strongly demonstrate that the nanofluid exhibits superior performance in terms of both temperature gain and thermal efficiency compared to classical fluids.

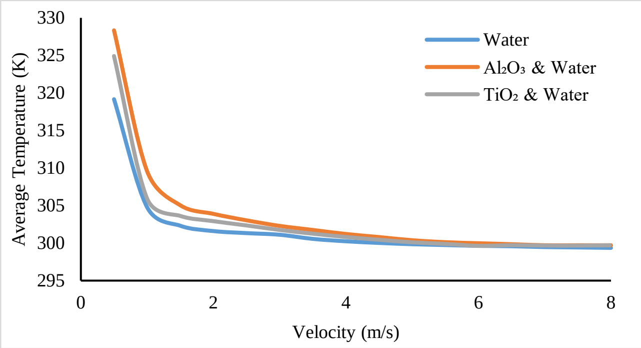

Figure 10 Average liquid outlet temperature at different flow rates

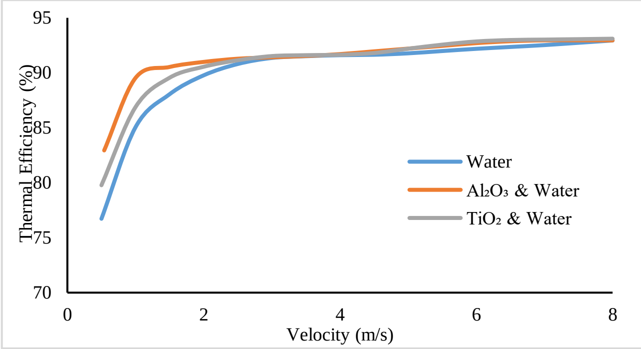

Figure 11 Thermal efficiency at different flow rates

As can be seen in Figure 10 and Figure 11, increasing velocity from 0.1 m/s to 8 m/s had significant effect on both the average outlet temperature and thermal efficiency. For example, the average outlet temperature of 310 K at at 0.1 m/s reached 335 K at 8 m/s.

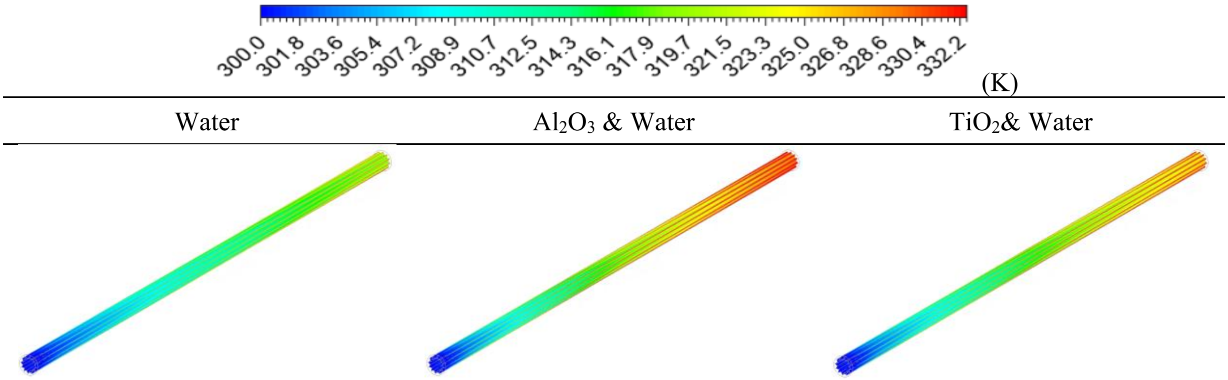

Figure 12 Temperature distribution along the pipe length for different fluids

Figure 12 compares the temperature distribution along the pipe length and shows that TiO_2/water and Al_2O_3/water nanofluids offer higher and more uniform temperature profiles compared to pure water. In TiO_2-enhanced systems, the temperature distribution is more homogeneous, with approximately 8–10 K higher temperatures achieved at the outlet.

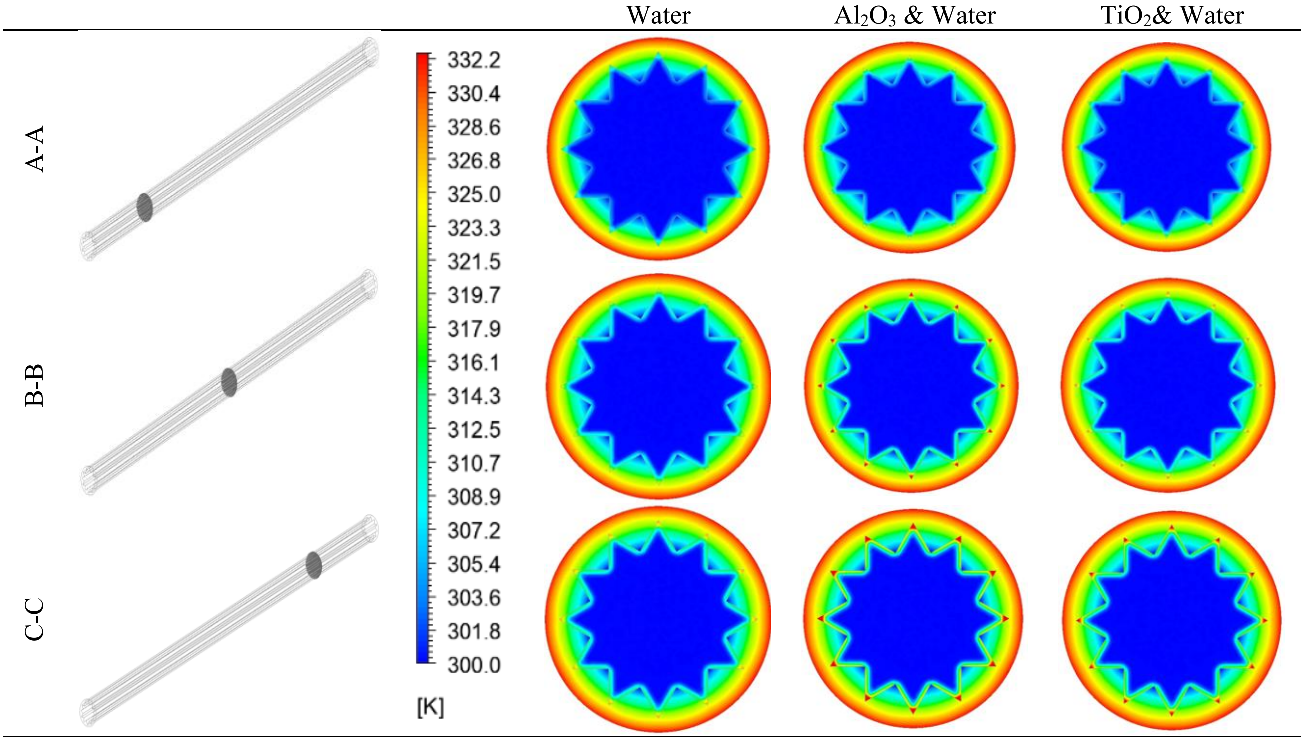

Figure 13 Temperature distribution in different fluids and at different sections

In Figure 13, when the temperature distributions at different cross-sections (A-A, B-B, C-C) were examined, a more stable and uniform thermal profile was observed in the systems using nanofluids. This situation indicates that the temperature gradients developing in the thermal boundary layer of the system are suppressed by the effect of nanoparticles, and the conductivity is increased.

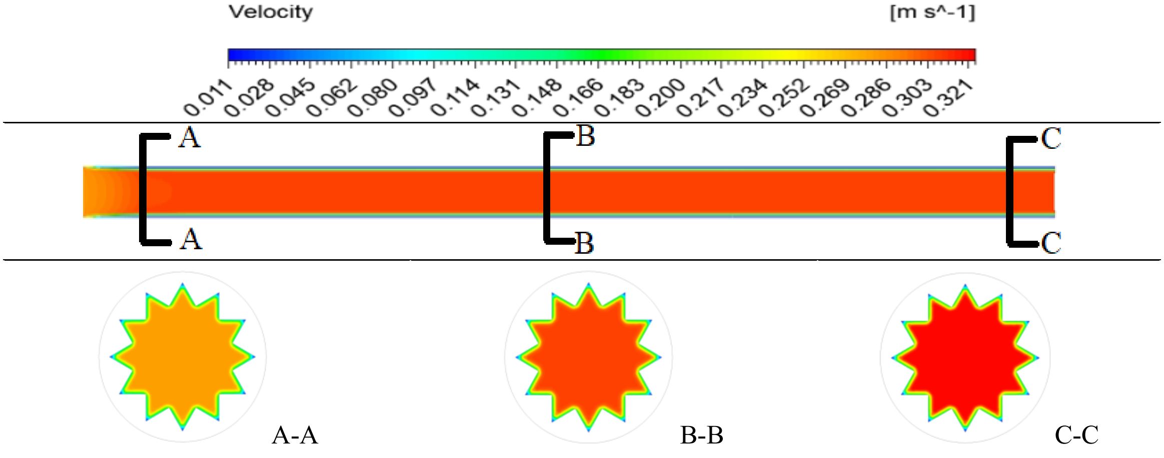

Figure 14 Fluid velocity distribution for water along the pipe at different cross-sectional areas

In Figure 14, the fluid velocity distribution along the pipe and at different cross-sections was examined; it was determined that nanofluids create a more stable and directed velocity profile despite the increase in viscosity. This is a positive development in terms of hydraulic stability and also contributes to the system's more efficient operation by reducing energy losses. All these analyses confirm that the nanofluid additive enhances system performance multidimensionally in terms of both thermal and fluid dynamics.

While the single-phase modeling approach utilized in this study does not capture micro-scale interactions, nanoparticles also contribute to improved thermal transport through mechanisms such as Brownian motion. The chaotic movement of nanoparticles, including Brownian motion, induces micro-convection within the fluid and thereby disrupts the growth of the thermally insulating boundary layer at the tube wall. This mechanism brings about better mixing between the hotter fluid near the wall and the cooler fluid at the core. This effect, combined with the inherently higher thermal conductivity of the solid nanoparticles compared to the base fluid, creates a more efficient "thermal bridge" for heat dissipation.

4. Conclusion

This study numerically investigated the impact of water-based TiO_2 and Al_2O_3 nanofluids on the thermo-hydraulic performance of a parabolic trough solar collector (PTSC). Based on the three-dimensional CFD simulations, the principal findings are summarized as follows:

- The application of TiO_2 /water nanofluid yielded an average outlet temperature increase of 7−10°C compared to the base fluid, which corresponds to a 10−12% enhancement in heat transfer efficiency.
- Increasing the nanoparticle volume fraction from 0.01% to 0.05% raised the overall thermal efficiency from 56% to 68%, primarily due to the enhanced thermal conductivity of the suspension.
- While thermal efficiency scales with particle concentration, the performance gains exhibit saturation; factoring in the hydraulic penalty of increased viscosity, the optimal volume fraction was determined to be in the range of 0.03%–0.05%.
- The integration of nanofluids facilitated a more uniform temperature distribution and a stable velocity profile along the absorber tube, reducing thermal gradients that could otherwise impact system life.

Limitations

While the present numerical study addresses the thermal performance enhancement of parabolic solar collectors using TiO_2 and Al_2O_3 nanofluids, its scope and conclusions are subject to several limitations that must be acknowledged:

- The study is based on a single-phase modeling approach that assumes the nanofluid to be a homogeneous continuum. Micro-scale phenomena such as Brownian motion, thermophoresis, and the potential velocity slip between the nanoparticles and the fluid were not considered.
- Despite the well-established governing equations and thermophysical property models derived from reputable experimental correlations, the final simulation results have not been validated against experimental data obtained from an identical physical setup.
- Although operation conditions in real-world applications are transient, the simulations were performed under steady-state conditions with idealized boundary conditions.

- The numerical model does not address long-term practical challenges associated with the use of nanofluids, such as nanoparticle agglomeration and sedimentation or the potential adverse effects like erosion of the absorber tube's inner surface due to particle motion.

Future Research

Based on the findings and limitations of the study, future research on implementation of nanofluids in PTSC systems may include, but is not limited to, the following:

- A laboratory-scale PTSC test rig can be built to measure the thermal performance with water-based TiO_2 and Al_2O_3 nanofluids under controlled conditions.
- Future computational studies can employ more sophisticated two-phase models like Mixture or Eulerian-Eulerian models for the effects of slip velocity mechanisms and nanoparticle migration.
- The potential of hybrid nanofluids consisting of a composite of two or more different nanoparticle types can be investigated.
- A cost-benefit analysis can be performed to determine optimum concentrations.
- Transient simulations can be conducted to better reflect real-world conditions.
- Techno-economic and life-cycle analyses can be performed to assess the commercial viability and long-term impacts, such as stability, maintenance, and durability.

Conflict of interest

The authors declare that they have no conflict of interest.

Author Contributions

MKY: Conceptualization, investigation, methodology, data curation, writing—original draft, writing—review and editing; **MM**: Conceptualization, investigation, methodology, data curation, software, visualization, writing—original draft.

References

[1] Ndede CO, Abonyo JO, Ojiambo V, Ochola JN. Numerical study of unsteady MHD flow of Cu–TiO2/water hybrid nanofluid in a parabolic solar collector with heat and mass transfer. *Modeling Earth Systems and Environment* (2025) **11**(1):58. doi:10.1007/s40808-024-02244-4.

[2] Hafeez M, Krawczuk M, Jamshed W, Din EE, Khalifa H-W, ElSeabee FAA. Thermal energy development in magnetohydrodynamic flow utilizing titanium dioxide, copper oxide and aluminum oxide nanoparticles: Thermal dispersion and heat generating formularization. *Frontiers in Energy Research* (2022) **10**:1000796.

[3] Dehaj MS, Mohiabadi MZ. Experimental investigation of heat pipe solar collector using MgO nanofluids. *Solar Energy Materials and Solar Cells* (2019) **191**:91–99. doi:10.1016/j.solmat.2018.10.025.

[4] Mburu ZM, Mondal S, Sibanda P, Sharma R. A numerical study of entropy generation on Oldroyd-B nanofluid flow past a Riga plate. *Journal of Thermal Engineering* (2021) **7**(4):845–866.

[5] Singh S, Mausam K, Ghosh SK, Tiwari AK. An experimental and numerical approach for thermal performance investigation of solar flat plate collector. *Environmental Science and Pollution Research* (2023) **30**(40):92859–92879.

[6] Pise GA, Salve SS, Pise AT, Pise AA. Investigation of solar heat pipe collector using nanofluid and surfactant. *Energy Procedia* (2016) **90**:481–491.

[7] Cho C-C. Influence of magnetic field on natural convection and entropy generation in Cu–water nanofluid-filled cavity with wavy surfaces. *International Journal of Heat and Mass Transfer* (2016) **101**:637–647.

[8] Yan S-R, Pordanjani AH, Aghakhani S, Goldanlou AS, Afrand M. Managment of natural convection of nanofluids inside a square enclosure by different nano powder shapes in presence of Fins with different shapes and magnetic field effect. *Advanced Powder Technology* (2020) **31**(7):2759–2777.

[9] Mahmoudi A, Mejri I, Abbassi MA, Omri A. Lattice Boltzmann simulation of MHD natural convection in a nanofluid-filled cavity with linear temperature distribution. *Powder Technology* (2014) **256**:257–271.

[10] Pordanjani AH, Raisi A, Ghasemi B. Numerical simulation of the magnetic field and Joule heating effects on force convection flow through parallel-plate microchannel in the presence of viscous dissipation effect. *Numerical Heat Transfer, Part A: Applications* (2019) **76**(6):499–516.

[11] Pordanjani AH, Vahedi SM, Aghakhani S, Afrand M, Öztop HF, Abu-Hamdeh N. Effect of magnetic field on mixed convection and entropy generation of hybrid nanofluid in an inclined enclosure: sensitivity analysis and optimization. *The European Physical Journal Plus* (2019) **134**:1–20.

[12] Mustafaoğlu M, Yeşilyurt MK, Acar M, Öner İV. Enhanced PEM fuel cell cooling using Al_2O_3 and TiO_2 nanofluid-based thermal models. *MANAS Journal of Engineering* (2026) **14**(1):30–43. doi:10.51354/mjen.1769337.

[13] Das SK, Choi SU, Yu W, Pradeep T. *Nanofluids: science and technology*: John Wiley & Sons (2007).

[14] Saghir MZ, Ahadi A, Mohamad A, Srinivasan S. Water aluminum oxide nanofluid benchmark model. *International Journal of Thermal Sciences* (2016) **109**:148–158. doi:10.1016/j.ijthermalsci.2016.06.002.